Bifurcation analysis of two coupled periodically driven Duffing oscillators

J. Kozłowski
Institute of Physics, University of Szczecin, ulica Wielkopolska 15, 70-451 Szczecin, Poland

U. Parlitz and W. Lauterborn
Institut für Angewandte Physik, Technische Hochschule Darmstadt, Schloßgartenstraße 7, D-64289 Darmstadt, Germany
(Received 11 July 1994)

Bifurcation diagrams and phase diagrams of two coupled periodically driven identical Duffing oscillators are presented. It is shown that the global pattern of bifurcation curves in parameter space consists of repeated subpatterns similar to the superstructure observed for single, periodically driven, strictly dissipative oscillators. The subpattern itself, however, is different from that of a single Duffing oscillator due, in particular, to Hopf bifurcations that are newly added to the bifurcation scenario.

PACS number(s): 05.45.+b, 47.52.+j, 46.10.+z, 02.30.Hq

I. INTRODUCTION

Coupled oscillators play an important role in different scientific disciplines, e.g. biology, electronics, and physics. Since the type of the oscillators, the type and topology of coupling, and the external perturbations including driving may be different, a large variety of coupled systems exists. The (individual) oscillators may roughly be divided into two classes: self-excited oscillators, which possess a stable limit cycle without external driving, and strictly dissipative oscillators, which converge to the quiescent state when not driven.

Self-excited oscillators (also called limit-cycle oscillators) can approximately be decribed by phase models. Using this idealization, large arrays of coupled oscillators have been investigated with respect to synchronization phenomena [1] or the occurrence of collective frequencies [2]. In some cases such systems admit the application of methods from statistical mechanics [3,4] and may also be modeled by coupled circle or torus maps [5].

The oscillators investigated in this paper are strictly dissipative and externally driven. Coupled systems using this type of oscillator have been investigated in the literature less intensely than self-excited models. In Ref. [6] the transition to hyperchaos for a system of coupled Duffing oscillators was studied and in Ref. [7] synchronization phenomena for different types of coupled systems were investigated. Furthermore, nonlinear resonances and bifurcation scenarios of a chain of coupled Toda oscillators were studied in detail by Geist and Lauterborn [8–10] and a chain of coupled Duffing oscillators was investigated by Dressler and Lauterborn with special attention paid to symmetry properties of the Lyapunov spectrum [11] and Ruelle's rotation number [12]. Umberger *et al.* [13] observed domainlike spatial structures in a chain of driven Duffing oscillators.

The symmetry properties of different coupling schemes are an important feature, which may drastically change the bifurcation structure of the coupled system. In particular, for electronic oscillators, symmetry problems have been studied extensively by Ashwin and Swift [14,15]. Since the driving force of the system investigated in this paper acts on one oscillator only, all coupling symmetries are broken.

Other interesting topics in the field of coupled oscillators are universal scaling features [16], the energy exchange between coupled oscillators [17], the dynamics of coupled conservative oscillators [18], and, for practical applications, arrays of coupled Josephson junctions [19,20].

In the following, we discuss some bifurcation properties of two mutually coupled, identical Duffing oscillators that are driven by an external sinusoidal force. Special attention will be paid to those features of the bifurcation structure that are similar to the typical bifurcation pattern found for single Duffing oscillators [21–26] and other nonlinear oscillators [27]. Many features of these strictly dissipative oscillators can be modeled by a special type of two-dimensional map [22].

The system that we are investigating is given by the following system of equations:

$$\begin{aligned}
\dot{y}_1 &= y_2, \\
\dot{y}_2 &= -dy_2 - y_1 - y_1^3 + c(y_3 - y_1) + f\cos(2\pi y_5), \\
\dot{y}_3 &= y_4, \\
\dot{y}_4 &= -dy_4 - y_3 - y_3^3 - c(y_3 - y_1), \\
\dot{y}_5 &= \omega/2\pi.
\end{aligned} \tag{1}$$

The state space is $R^4 \times S^1$, i.e., y_5 is always considered mod 1 giving a cyclic variable $y_5 \in [0,1]$.

The frequency ω and the amplitude f of the driving force are used as control parameters in the bifurcation diagrams and phase diagrams that will be presented in the following. For all examples we chose the fixed damping parameter $d = 0.1$ and the coupling constant $c = 5$.

Due to the linear coupling and the symmetric potential of both oscillators, the coupled system (1) possesses the same symmetry properties as a single Duffing oscillator

[22]. Therefore, not only may saddle-node (sn), period-doubling (pd), and Hopf bifurcations (H) occur in the coupled system (1), but also symmetry-breaking (sb) bifurcations. As in the case of a single Duffing oscillator, only asymmetrical orbits can undergo period-doubling bifurcations.

For better visualization of the attractors and their bifurcations the dynamics is investigated in the Poincaré section defined by

$$\Sigma = \{(y_1, y_2, y_3, y_4, y_5) \in R^4 \times S^1 : y_5 = \text{const}\}. \quad (2)$$

The coordinates of the four-dimensional Poincaré cross section Σ will be called u_i in the following.

II. BIFURCATION DIAGRAMS

In order to investigate the dependence of the system on a single control parameter (here, the frequency ω of the driving force), several bifurcation diagrams have been computed. Each bifurcation diagram is calculated by increasing and decreasing the value of the control parameter in small steps. The step size has been varied from 0.01 to 0.0001. The last computed u_i values (for a particular ω value) are used as a new set of initial values for the next ω value. The bifurcation diagrams given show the projection of the attractors in the Poincaré section onto the u_1 or the u_2 coordinate versus the control parameter ω.

In the following we will show a sequence of diagrams for increasing driving amplitude f. Figure 1 shows a bifurcation diagram for a comparatively small driving amplitude of $f = 2$. Different resonances and sn bifurcations occur and a pair of sb bifurcations near $\omega = 2.1$. At $\omega \approx 3.95$ a Hopf bifurcation takes place and quasiperiodic as well as chaotic attractors occur. This bifurcation scenario will be discussed in more detail in Sec. IV. When the driving amplitude f is increased, sb bifurcations occur between further resonances. As an example, Fig. 2 shows the occurrence of a second pair of sb bifurcations near $\omega = 0.8$ for $f = 3$. In the following each pair of sb bifurcations will be abbreviated as -(sb-sb)-. The notation -(sb-sb)- means that there are two parameter values where symmetry-breaking bifurcations take place: the first one, where a symmetrical periodic solution splits into two coexisting asymmetrical attractors (branches), and the second one, where these two

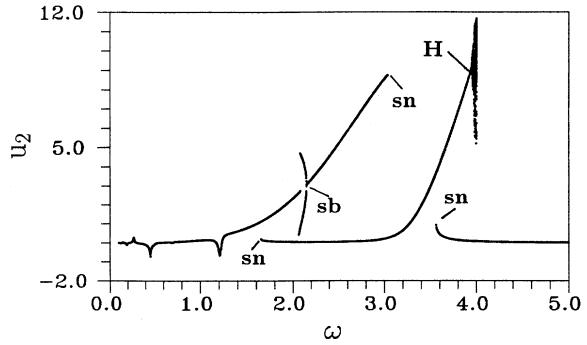

FIG. 1. Bifurcation diagram for the driving amplitude $f = 2$ showing the second coordinate u_2 of the Poincaré section vs the driving frequency ω. Several resonances and a pair of symmetry-breaking bifurcations at $\omega \approx 2.1$ occur. Near $\omega = 3.95$ a Hopf bifurcation takes place.

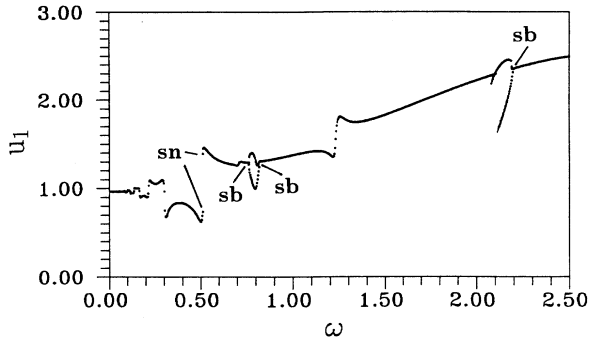

FIG. 2. Bifurcation diagram for the driving amplitude $f = 3$ showing the first coordinate u_1 of the Poincaré section vs the driving frequency ω. At $\omega \approx 0.8$ and $\omega \approx 2.15$ pairs -(sb-sb)- of symmetry-breaking bifurcations occur.

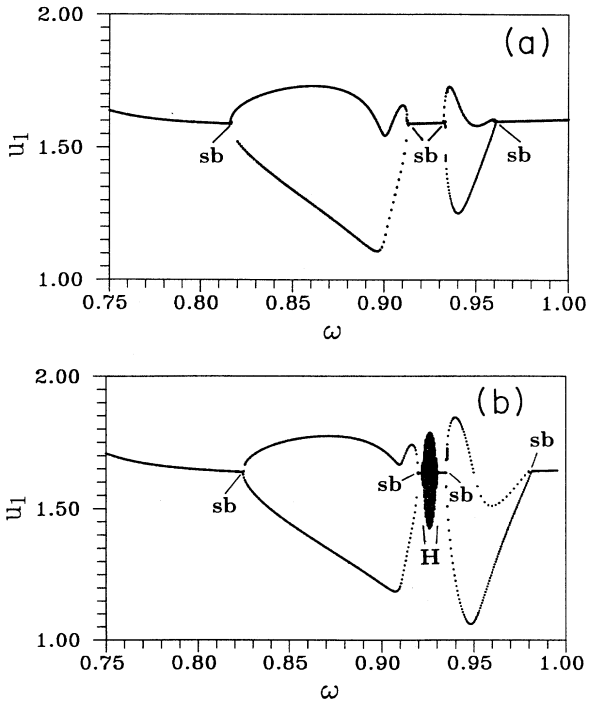

FIG. 3. Bifurcation diagrams for the driving amplitude $f = 4.5$ and $f = 4.8$. (a) $f = 4.5$. Near the -(sb-sb)- region at $\omega \approx 0.8$ for $f = 3$ shown in Fig. 2, another -(sb-sb)-bifurcation occurs at $\omega \approx 0.93$. (b) $f = 4.8$. In the frequency region between the two -(sb-sb)- bifurcation regions additional Hopf bifurcations -(H-H)- and thereby quasiperiodic attractors and periodic windows occur.

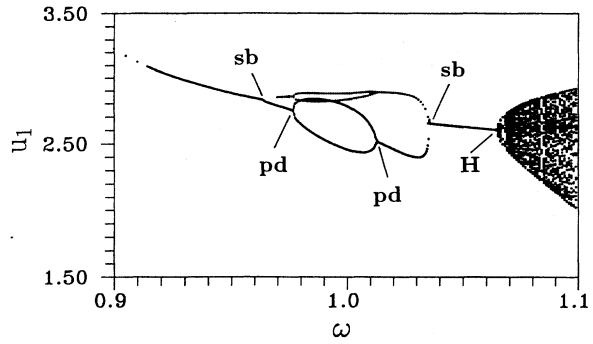

FIG. 4. Bifurcation diagram for $f = 17$. A period-doubling (pd) bifurcation occurs in the parameter region where the symmetry is broken.

attractors (branches) join, again forming a symmetrical period-one solution.

For $f = 4.5$ we observe that a sequence of two pairs of symmetry-breaking bifurcations -(sb-sb)-(sb-sb)- occurs as can be seen in Fig. 3(a). When the amplitude is increased further to $f = 4.8$, between the two pairs of symmetry-breaking bifurcations an additional pair of Hopf bifurcations occurs, as can be seen in Fig. 3(b). As we shall see later on, the sequence -(sb-sb)-(H-H)-(sb-sb)- is a characteristic feature of the bifurcation structure of this system.

In the -(sb-sb)- regions period-doubling and further Hopf bifurcations emerge with increasing f. As an example we consider the symmetry-breaking bifurcation to the left of the Hopf bifurcation shown in Fig. 3(b). Figure 4 shows, for $f = 17$, a sequence -sb-(pd-pd)-sb- consisting of a symmetry-breaking, a period-doubling, a reversed period-doubling, and a reversed symmetry-breaking bifurcation. When the amplitude reaches the value $f = 19$, in the middle of the period-two region another Hopf bifurcation takes place, as shown in Fig. 5 for $f = 20$. Windows of periodic solutions separated by quasiperiodic

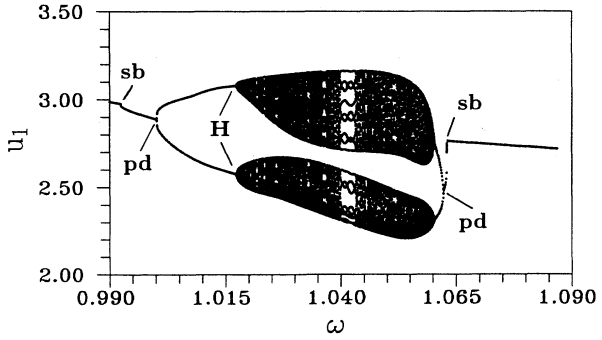

FIG. 5. Bifurcation diagrams for $f = 20$. In the period–doubling region shown in Fig. 4 a Hopf bifurcation occurs and in the quasiperiodic region thus generated high-periodic orbits appear.

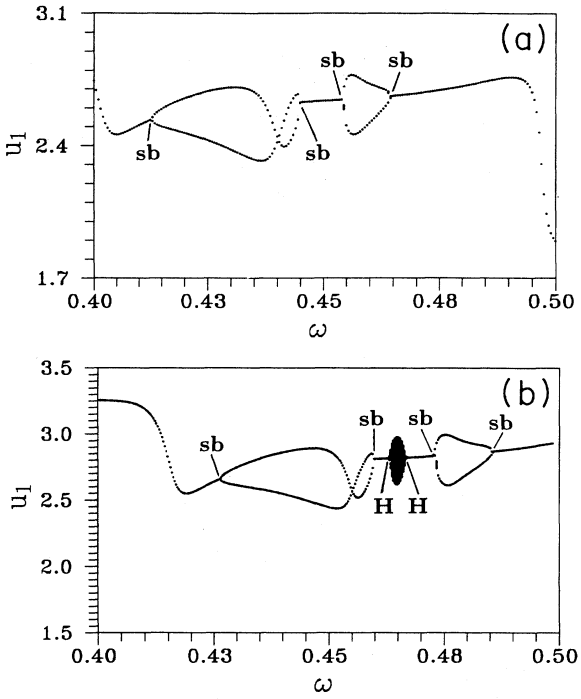

FIG. 6. Bifurcation diagrams for (a) $f = 20$ and (b) $f = 25$ showing the occurrence of a bifurcation sequence -(sb-sb)-(H-H)-(sb-sb)- near $\omega \approx 0.45$ that is similar to that shown in Fig. 3.

oscillations are clearly visible. The Poincaré sections of the quasiperiodic attractors in this case consist of two invariant circles.

For $f = 20$, in another ω region, a pair of two symmetry-breaking bifurcations occurs [see Fig. 6(a)] and again a Hopf bifurcation emerges when the driving amplitude f is increased further [Fig. 6(b)]. Comparing Fig. 6 with Fig. 3 we recognize that both diagrams show, for different frequency regions, the same structure (sb-sb)-(H-H)-(sb-sb), consisting of symmetry-breaking and Hopf bifurcations. This bifurcation sequence turned out to be one building block of a recurring pattern of bifurcations. A corresponding superstructure of the bifurcation set is well known for single oscillators [21,22,27] and can best be visualized using phase diagrams.

III. PHASE DIAGRAMS

Phase diagrams show bifurcation points, curves, or even surfaces in parameter space. As an example, Fig. 7 shows the phase diagram of the single Duffing oscillator

$$\ddot{y} + d\dot{y} + y + y^3 = f\cos(\omega t). \tag{3}$$

As can be seen in Fig. 7, the bifurcation structure consists of repeated subpatterns of sn, sb, and pd horns. Inside the pd horns, further period-doubling bifurcations take place and chaotic attractors occur [22]. In the case of the coupled Duffing oscillators (1), the bifurcation structure

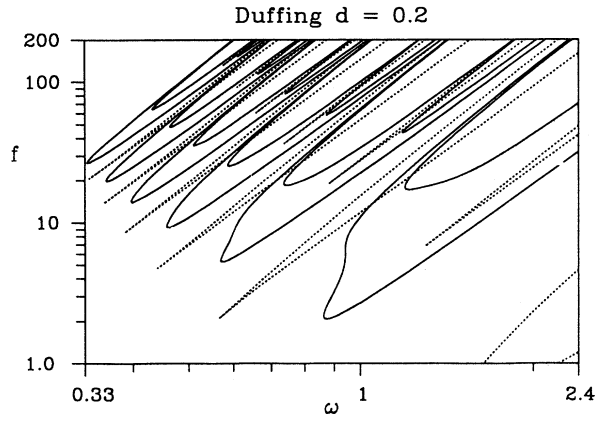

FIG. 7. Phase diagram of the single Duffing oscillator (3) on a logarithmic scale for $d = 0.2$ showing sn, sb, and pd bifurcation curves. The sn curves are drawn as dotted lines. The sb curves are those solid curves embracing the inner ones.

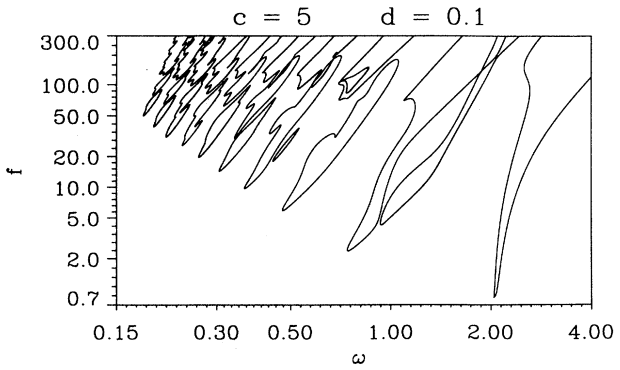

FIG. 9. Phase diagram of the two coupled Duffing oscillators (1) showing symmetry-breaking (sb) bifurcation curves.

is more complicated than that of a single oscillator because additionally Hopf bifurcation curves occur. Figures 8, 9, and 10 show sn, sb, and Hopf bifurcation curves of the coupled Duffing oscillators (1), respectively. Again we observe a repeated occurrence of the sn, sb, and H bifurcation curves. However, the curves corresponding in particular to the first resonances (i.e., for large and medium ω values) are rather distorted and do not resemble each other very much. Furthermore, the diagrams may partly be incomplete in spite of an extensive search for missing bifurcation curves. For a single Duffing oscillator (3) some asymptotic patterns of bifurcation curves exist in the limit $\omega \to 0$ with sufficiently small damping. This can already be seen in Fig. 7 and was proved by Eilenberger and Schmidt [23]. From the results obtained so far we conjecture that a similar property also exists for the coupled system (1). For better visualization Fig. 11 shows, for small driving frequencies, a phase diagram with sb and sn bifurcation curves only. One can see that the global bifurcation set of the two coupled Duffing oscillators (1) consists of repeated and slightly distorted copies of some basic patterns that become more and more similar for decreasing driving frequencies.

A first hint at the mathematical structure underlying this pattern can be found when investigating the topology of the flow for very small amplitudes of the oscillation. The local bifurcations studied in this paper are given by the eigenvalues of the linearized Poincaré map DP of the system that can be obtained by integrating the matrix variational equation

$$\dot{Y} = Dv(\mathbf{y})Y, \tag{4}$$

where the matrix

$$Dv(\mathbf{y}) = \begin{pmatrix} 0 & 1 & 0 & 0 \\ -1-y_1^2-c & -d & c & 0 \\ 0 & 0 & 0 & 1 \\ c & 0 & -1-y_3^2-c & -d \end{pmatrix} \tag{5}$$

describes the vector field linearized along the solution $\mathbf{y}$ and $Y(t)$ is a 4×4 matrix. When using the unit matrix I as the initial condition $Y(0) = I$, the resulting solution $Y(T)$ after one period T of the oscillation represents the linearized Poincaré map DP. For very small amplitudes

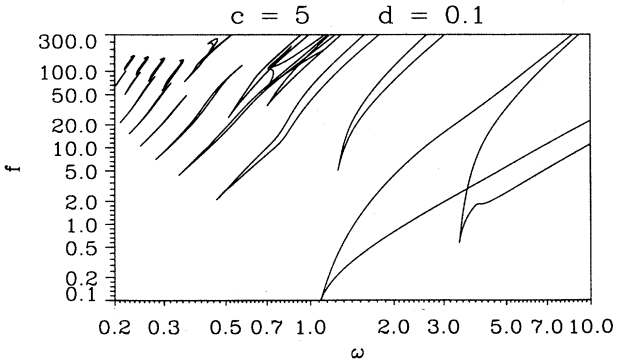

FIG. 8. Phase diagram of the two coupled Duffing oscillators (1) showing saddle-node (sn) bifurcation curves.

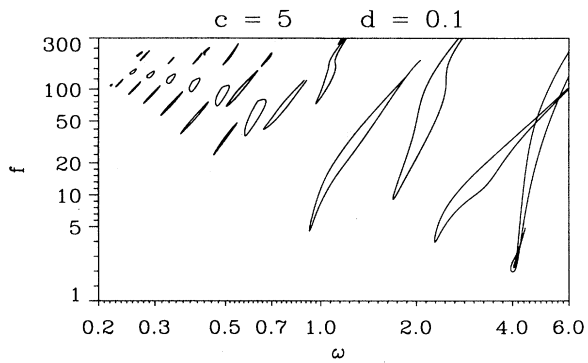

FIG. 10. Phase diagram of the two coupled Duffing oscillators (1) showing Hopf bifurcation curves.

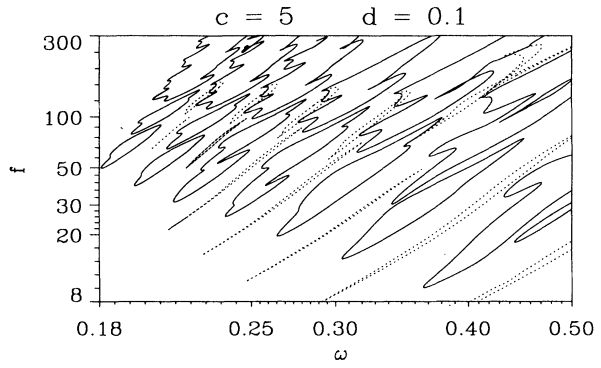

FIG. 11. Phase diagram showing the (asymptotic) bifurcation structure of the two coupled Duffing oscillators (1) for small driving frequencies. The sb and sn bifurcation curves shown are plotted as solid and dotted lines, respectively.

y_1 and y_3, the quantities y_1^2 and y_3^2 in the matrix Dv may be neglected. In this case the solution of Eq. (4) is given by

$$Y(t) = Y_0 \exp(tA), \tag{6}$$

where the time-independent matrix A equals $Dv(\mathbf{0})$ and the matrix $Y(0) = Y_0$ contains the initial conditions. Let $\mu_k = \lambda_k + i\Omega_k$ $(k = 1,2,3,4)$ be the eigenvalues of the matrix A. Then the eigenvalues of the linearized Poincaré map DP may be written as

$$\sigma_k = e^{T\mu_k} = e^{T\lambda_k}[\cos(T\Omega_k) + i\sin(T\Omega_k)]. \tag{7}$$

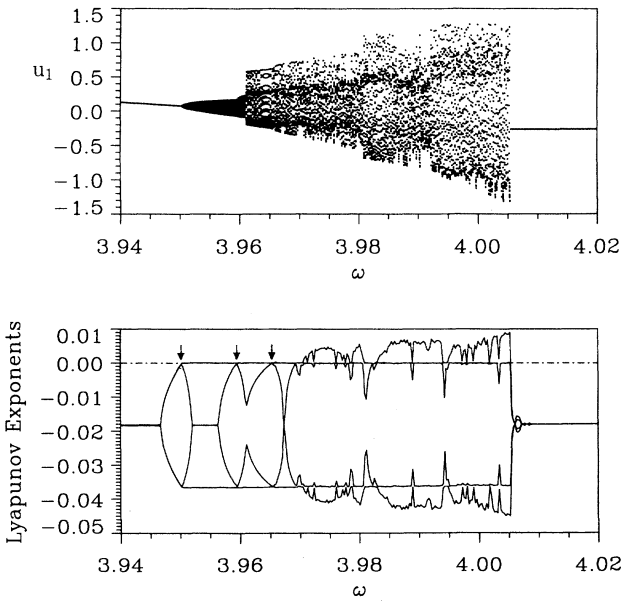

FIG. 12. Bifurcation diagram and Lyapunov exponents of the coupled Duffing oscillators (1) for $f = 2$ showing a quasiperiodic route to chaos. The Lyapunov exponents are those of the Poincaré map, i.e., another vanishing exponent exists. Therefore, for the ω values denoted by the arrows, *two* Lyapunov exponents are zero.

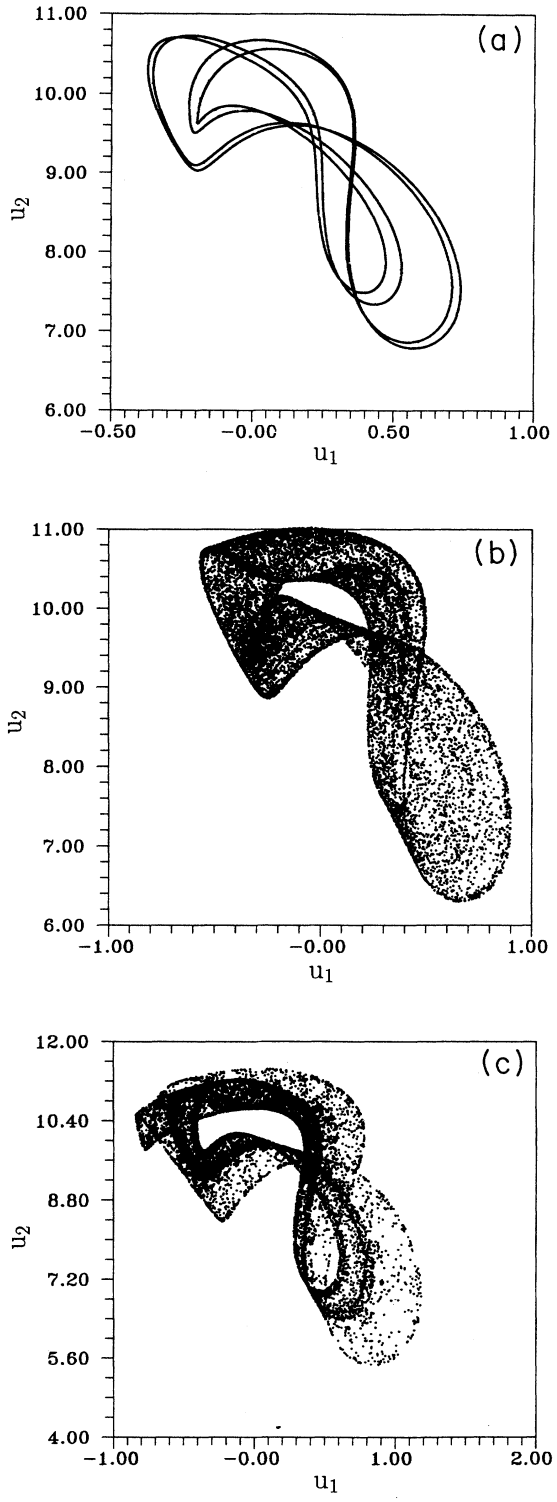

FIG. 13. Typical attractors for $f = 2$, $c = 5$, $d = 0.1$, and ω values from the bifurcation diagram shown in Fig. 12. Shown is the projection of the attractors in the Poincaré section onto the first two coordinates of the Poincaré section. The two chaotic attractors shown in (b) and (c) possess two vanishing exponents and one positive Lyapunov exponent (see Fig. 12). (a) $\omega = 3.97$, three-torus. (b) $\omega = 3.98$, chaotic attractor. (c) $\omega = 3.99$, chaotic attractor (note the different scale).

Since for stable solutions the real part λ_k is negative, these eigenvalues spiral into the origin of the complex plane when the driving frequency $\omega = 2\pi/T$ is decreased. In particular the eigenvalues equal positive and negative real numbers in an alternating way. For larger values of the driving amplitude f the influence of the nonlinearities becomes more important and the eigenvalues move toward the critical values $+1$ (sn bifurcation) or -1 (pd bifurcation). This leads, for systems without any symmetries, to a pattern of alternating sn- and pd-bifurcation curves in parameter space [27]. In the case of the coupled Duffing oscillators (1) the symmetry of their potentials implies the existence of a root $\tilde{P} = -H$ of the Poincaré map $P = \tilde{P} \circ \tilde{P} = (-H)^2$, where the map H is obtained by integrating the variables of the Poincaré map over half a period of the oscillation. After linearization the eigenvalues of the linearized map DH also spiral into the origin of the complex plane when the driving frequency ω is decreased. For increasing driving amplitude f the eigenvalues (may) converge again to the critical values $+1$ and -1. However, an eigenvalue of $+1$ (-1) of DH implies an eigenvalue of -1 $(+1)$ for the root $D\tilde{P}$ and therefore leads to an eigenvalue of $(-1)^2$ $[(+1)^2]$ for the linearized Poincaré map DP. Therefore, an alternating sequence of symmetry-breaking bifurcations $[(-1)^2 = 1]$ and saddle-node bifurcations $[(+1)^2 = 1]$ has to be expected. Furthermore, this simple linear analysis indicates that a similar eigenvalue scenario and the resulting alternating bifurcation sequences have to be expected for all systems of coupled strictly dissipative oscillators that are driven periodically.

IV. QUASIPERIODICITY AND CHAOTIC ATTRACTORS

Two routes to chaos have been observed so far for the two coupled Duffing oscillators (1). The first is the well known period-doubling cascade that occurs in parameter regions where the symmetry of the attractors is broken. The first two steps of such a cascade are shown, for example, in Fig. 4. However, in contrast to the single Duffing oscillator (where Hopf bifurcations are not possible), period doubling is not the only route to chaos. Figure 12 shows a bifurcation diagram and the parameter dependence of the corresponding Lyapunov exponents for $f = 2$, where a quasiperiodic route to chaos occurs (compare Fig. 1). Since the Lyapunov exponents given are those of the Poincaré map, another vanishing exponent exists. At $\omega \approx 3.97$ a quasiperiodic attractor with three incommensurate frequencies (a three-torus) occurs and at $\omega = 3.98$ and $\omega = 3.99$, for example, chaotic attractors with one positive Lyapunov exponent and two exponents equal to zero occur. Projections of the Poincaré sections of the corresponding attractors are shown in Fig. 13.

It is somewhat surprising to observe such a high-dimensional chaotic attractor for a small driving amplitude ($f = 2$). This value is far below the threshold for the first period doubling of the coupled system (1) as well as for the single oscillator (3). Another interesting feature is that over almost the whole interval from $\omega = 3.95$ to $\omega = 4.005$ two vanishing Lyapunov exponents occur. The investigation of details of the underlying bifurcation scenario is left to future work.

V. CONCLUSION

The structure of local bifurcations in the parameter space of two coupled Duffing oscillators has been investigated in terms of bifurcation diagrams and phase diagrams. It has been shown that the bifurcation structure consists of repeated subpatterns similar to the superstructure observed for single, periodically driven, Duffing oscillators. The basic pattern, however, is more complicated and additional Hopf bifurcations occur. Furthermore, Hopf bifurcations of period-two solutions, three tori, and chaotic attractors with two vanishing Lyapunov exponents have been observed. For a better understanding of the periodic superstructure in the bifurcation set more detailed numerical investigations are necessary. On the basis of the results obtained so far we conjecture that, analogous to the case of the single Duffing oscillator, some asymptotic bifurcation structures for $\omega \to 0$ and sufficiently small damping exists.

ACKNOWLEDGMENTS

J.K. thanks the Deutscher Akademischer Austauschdienst for financial support and for supporting this research and Professor W. Lauterborn and his nonlinear dynamics group at the University of Darmstadt for their hospitality. U.P. and W.L. acknowledge support by the DFG (Grant No. SFB 185/A7, Nichtlineare Dynamik).

[1] M. Tsodyks, I. Mitkov, and H. Sompolinsky, Phys. Rev. Lett. **71**, 1280 (1993).
[2] E. Niebur, H.G. Schuster, and D.M. Kammen, Phys. Rev. Lett. **67**, 2753 (1991).
[3] H. Daido, Physica D **69**, 394 (1993); Phys. Rev. Lett. **61**, 231 (1988); **68**, 1073 (1992).
[4] P.C. Matthews, R.E. Mirollo, and S.H. Strogatz, Physica D **52**, 293 (1991).
[5] C. Baesens, J. Guckenheimer, S. Kim, and R.S. MacKay, Physica D **49**, 387 (1991).
[6] T. Kapitaniak, Phys. Rev. E **47**, R2975 (1993).
[7] P.S. Landa and M.G. Rosenblum, Appl. Mech. Rev. **46**, 414 (1993).
[8] K. Geist and W. Lauterborn, Physica D **31**, 103 (1988).
[9] K. Geist and W. Lauterborn, Physica D **41**, 1 (1990).
[10] K. Geist and W. Lauterborn, Physica D **52**, 551 (1991).
[11] U. Dressler, Phys. Rev. A **38**, 2103 (1988).
[12] U. Dressler and W. Lauterborn, Phys. Rev. A **41**, 6702

(1990).
[13] D.K. Umberger, C. Grebogi, E. Ott, and B. Afeyan, Phys. Rev. A **39**, 4835 (1989).
[14] P. Ashwin, Nonlinearity **3**, 603 (1990).
[15] P. Ashwin and J.W. Swift, J. Nonlin. Sci. **2**, 69 (1992).
[16] F.H. Ling, G. Schmidt, and H. Kook, Int. J. Bifurcation Chaos **1**, 363 (1991).
[17] T. Eisenhammer, A. Hübler, T. Geisel, and E. Lüscher, Phys. Rev. A **41**, 3332 (1990).
[18] K.M. Atkins and D.E. Logan, J. Chem. Phys. **97**, 2438 (1992).
[19] K.Y. Tsang, R.E. Mirollo, S.H. Strogatz, and K. Wiesenfeld, Physica D **48**, 102 (1991).
[20] J.W. Swift, S.H. Strogatz, and K. Wiesenfeld, Physica D **55**, 239 (1992).
[21] S. Sato, M. Sano, and Y. Sawada, Phys. Rev. A **28**, 1654 (1983).
[22] U. Parlitz, Int. J. Bifurcation Chaos **3**, 703 (1992).
[23] G. Eilenberger and K. Schmidt, J. Phys. A **25**, 6335 (1993).
[24] V. Englisch and W. Lauterborn, Phys. Rev. A **44**, 916 (1991).
[25] Y. Ueda, Chaos, Solitons Fractals **1**, 199 (1991).
[26] H.G. Solari and R. Gilmore, Phys. Rev. A **38**, 1566 (1988)
[27] C. Scheffczyk, U. Parlitz, T. Kurz, W. Knop, and W. Lauterborn, Phys. Rev. A **43**, 6495 (1991).